Low Solubility of Alumina in Enstatite and Uncertainties in Estimated Palaeogeotherms

Susan Howells and M. J. O'Hara

Phil. Trans. R. Soc. Lond. A 1978 **288**, 471-486
doi: 10.1098/rsta.1978.0029

Phil. Trans. R. Soc. Lond. A. **288**, 471–486 (1978) [471]
Printed in Great Britain

Low solubility of alumina in enstatite and uncertainties in estimated palaeogeotherms

BY SUSAN HOWELLS AND M. J. O'HARA
Grant Institute of Geology, Edinburgh University, West Mains Road,
Edinburgh EH9 3JW, U.K.

Spurious kinks in estimated palaeogeotherms may result from small errors in the calibration of the geothermometers and geobarometers. New data indicate that the equilibrium solubility of alumina in enstatite is even less than shown by recent studies, and that the slopes ($\mathrm{d}T/\mathrm{d}P$) of the isopleths of equal alumina content are steeper than hitherto believed. Consequently, pressures of equilibration estimated from current formulations of the orthopyroxene–garnet geobarometer will be too high at high temperatures (> 1200 °C) and too low at low temperatures.

INTRODUCTION

The estimation of the pressures and temperatures of equilibration of mineral assemblages in suites of natural rocks can lead to the establishment of palaeogeotherms in the crust and upper mantle at times ranging back to the Archaean. When it is desired to establish palaeogeotherms in deep crust (granulite facies) and upper mantle (granulite–eclogite facies) rocks the results rely upon the correct interpretation of the temperature and pressure dependence of the distribution of certain elements between clinopyroxene, orthopyroxene, garnet, spinel and olivine.

This paper considers the experimental calibration of the clinopyroxene geothermometer (essentially the Ca/Mg ratio of clinopyroxene coexisting with enstatite) and the orthopyroxene geobarometer (essentially the Al_2O_3 content of orthopyroxene coexisting with garnet).

PALAEOGEOTHERMS

Estimates of upper mantle geotherms in the Mesozoic have been obtained from suites of garnet–peridotite nodules in kimberlite (e.g. Boyd 1973).

Temperature estimates were based upon the use of the Davis & Boyd (1966) experimental determination of diopside compositions coexisting with enstatite at 30 kbar† assuming no pressure effects on this solvus, negligible effects due to substitution of alumina in the pyroxenes and ignoring possible effects due to the substitution of Fe^{2+} for Mg^{2+} in the pyroxenes. An improved treatment which in principle allows for the effects of alumina and iron was proposed by Wood & Banno (1973), but was calibrated against the Davis & Boyd (1966) experimental data.

Pressure estimates were based upon the use of the Boyd & England (1964) or MacGregor (1974) experimental data for Al_2O_3 content of enstatites coexisting with pyrope in the system $MgO–Al_2O_3–SiO_2$. Most of these experiments were conducted on starting materials which were glass or derived by the devitrification or crystallization of glass in the presence of garnet seeds.

---

† 1 kbar = 10^8 Pa.

An improved treatment of pressure estimates allowing for the effects of chrome, iron and calcium in the natural minerals was developed by Wood & Banno (1973) and calibrated against the Boyd & England (1964) data. A revised version, calibrated against the MacGregor (1974) data was proposed by Wood (1974) with further adjustments to allow for the non-ideal behaviour of iron-bearing components, calibrated against synthesis experiments in which pyroxenes were grown at relatively low temperatures from glasses seeded with orthopyroxene.

A striking feature of most of the palaeogeotherms presented by Boyd (1973), MacGregor (1975) is the presence of a kink, i.e. a marked increase of the geothermal gradient, in the rocks derived from greatest depths.

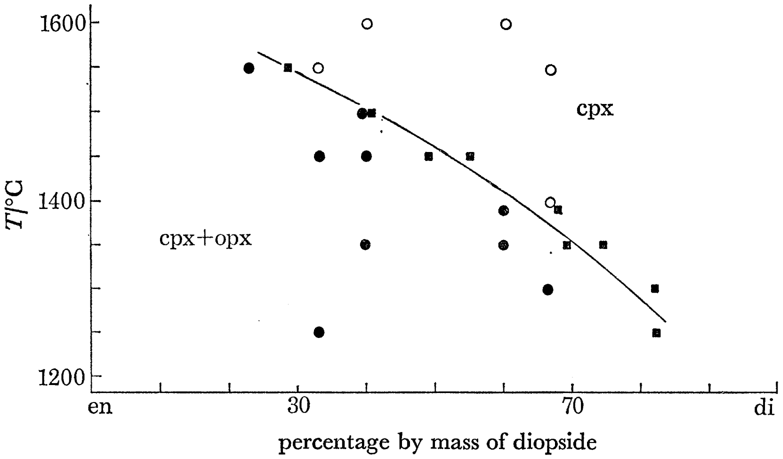

FIGURE 1. Results of homogenization experiments on mixtures of natural diopside and enstatite from a garnet–peridotite nodule (A3/10596) in kimberlite (for mineral analyses see O'Hara & Yoder 1967; for additional run details see Howells 1976). ○, homogenous clinopyroxene produced; ●, clinopyroxene+orthopyroxene; ■, composition of clinopyroxene in two phase run products by X-ray measurement (calibrated against homogeneous clinopyroxene run products).

GROUNDS FOR CAUTION: CALIBRATION UNCERTAINTIES AND SPURIOUS KINKS

Setting aside all arguments about whether a kink is really required by the data points, or how it should be interpreted, several considerations indicated the need for caution in accepting the specific temperatures and pressures indicated for the palaeogeotherms.

Data (figure 1) for the diopside–enstatite solvus obtained by homogenizing a natural mineral pair from a nodule in kimberlite (O'Hara & Yoder 1967; amplified by Howells 1976) did not support the form of the solvus obtained by Davis & Boyd (1966) at high temperatures.

Results in which garnet had been dissolved into coexisting pyroxenes of a natural olivine–garnet websterite nodule from kimberlite (Howells, Begg & O'Hara 1975) indicated a much lower Al_2O_3 solubility (*ca.* 5.5 % by mass) in the enstatite at *ca.* 1500 °C than required by the results of Boyd & England (1964) or MacGregor (1974), yet solution of garnet into pyroxene appears to be a fast process in experiments of this type (Boyd & England 1964; MacGregor & Ringwood 1964; Howells *et al.* 1975).

No peridotites are known to us in which the original existence can be established of orthopyroxenes containing as much Al_2O_3 in solution as the maxima required by the results of Boyd & England (1964), MacGregor (1974), or more recently by Akella (1976).

A spurious kink may arise in the apparent geotherm if temperatures are estimated by reference to a working solvus which intersects the correct solvus in the manner shown in figure 2. Note that the estimated geotherm is less steep (lower $\mathrm{d}T/\mathrm{d}P$) than the correct one.

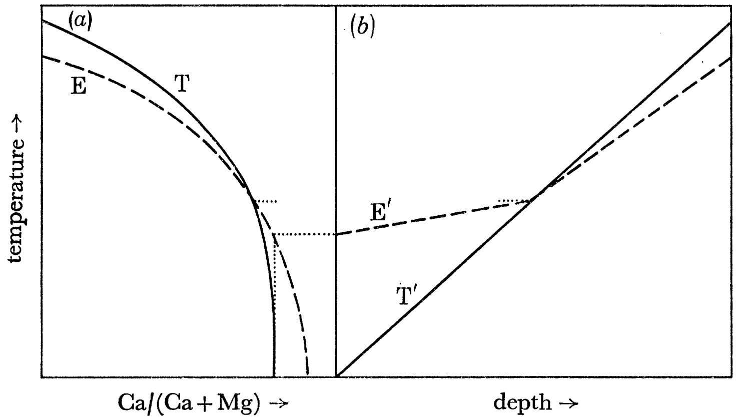

FIGURE 2. (*a*) Temperature–composition plot showing the true solvus limit, T, of diopside coexisting with enstatite relative to an erroneous solvus, E. (*b*) Temperature–depth plot showing the true geotherm, T′, and the estimated geotherm, E′, obtained if temperatures of mineral assemblages equilibrated along T′ are estimated using solvus E of (*a*) (depths (pressures) are assumed to have been correctly estimated in both cases).

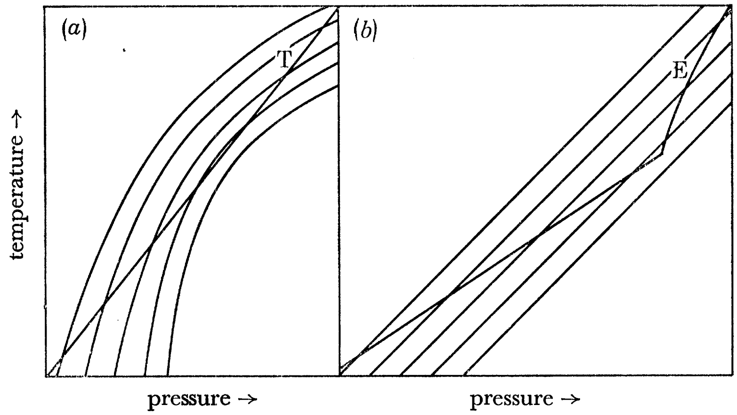

FIGURE 3. (*a*) Temperature–pressure plot showing ‘true’ curved isopleths of Al_2O_3 content in orthopyroxene coexisting with garnet, and, superimposed, a true geotherm T. (*b*) Temperature–pressure plot showing the geotherm, E, estimated from mineral assemblages equilibrated along the true geotherm of figure 3*a* if the isopleths of Al_2O_3 content in orthopyroxene are assumed, erroneously, to be linear.

A spurious kink similar in shape to that deduced by Boyd (1973) may also arise in the apparent geotherm if pressures are estimated by reference to a set of isopleths of Al_2O_3 content which are less markedly curved than the correct isopleths, as shown in figure 3. In this context it is worth noting that pressure estimates of Lesotho nodules (Boyd 1973) were based on straight line extrapolations (on P/T sections) of the Al_2O_3 content of experimentally produced enstatites to the much lower Al_2O_3 contents of the orthopyroxenes in the nodules.

REACTION CLINOPYROXENE + ORTHOPYROXENE = SUBCALCIC CLINOPYROXENE + GARNET, AND THE KINKED GEOTHERM

The existence of this reaction in olivine saturated assemblages of the system CaO–MgO–Al_2O_3–SiO_2 at *ca.* 1550 °C was indicated (O'Hara 1975) by synthesis experiments on a type A starting material (see table 2). An analogous reaction in natural peridotites could explain the bimodal distribution of Ca/(Ca + Mg + Fe) ratios of diopsides from nodules in kimberlite and the observation that whereas the more calcic diopsides have Mg/(Mg + Fe) ratios greater than in the coexisting enstatites, the subcalcic diopsides have Mg/(Mg + Fe) ratios lower than in the coexisting enstatites (also with a bimodal distribution rather than an evenly populated range). Such a reaction could also contribute to the appearance of spurious kinks in the apparent geotherms determined from orthopyroxene–clinopyroxene–garnet equilibria.

However, further experiments on this composition and on compositions with the same garnet–pyroxene component ratios but less forsterite, using starting materials analogous to types B_2, D_1 (as defined in table 2) and type D_1 recrystallized as type B_1, have indicated that the garnet solubility in the pyroxenes is lower than previously shown (and, therefore, much lower than implied by the results of Akella (1976)). Moreover, the abrupt change in the character of the clinopyroxenes above and below 1550 °C may reflect a change in the kinetics of garnet and pyroxene growth from type A material rather than the reaction sought. Further studies on this problem are in progress.

DIOPSIDE–ENSTATITE SOLVUS

A reinvestigation of the diopside–enstatite solvus above 1400 °C was carried out (Howells & O'Hara 1975; Howells 1976) at 20 and 30 kbar with four principal results:

(i) The solubility of enstatite in clinopyroxene was much less than indicated by Davis & Boyd (1966). The results are compatible with or in accord with those published previously by Nehru & Wyllie (1974), simultaneously by Mori & Green (1975) and subsequently by Mori & Green (1976) and Lindsley & Dixon (1976). These data combine (figure 4) to show that the diopside limb of the diopside–enstatite solvus crosses that obtained by Davis & Boyd (1966) in a manner which will contribute to the appearance of spurious kinks in published geotherms based on mineral equilibria in peridotite nodules in kimberlites, and will cause the estimated geotherm to be less steep than the true geotherm.

(ii) The solubility of enstatite in diopside is pressure dependent, being lower at higher pressures. This result was reported simultaneously by Mori & Green (1975) and confirmed by Lindsley & Dixon (1976) and Powell (1978). The effect of pressure on the apparent temperature estimated for the equilibration of a diopside–enstatite pair may be very large at low temperature where the effect of temperature is small (figure 4).

(iii) The field of two clinopyroxenes, and the stability of a magnesian pigeonite at 20 kbar, as reported by Kushiro (1969*a*), could not be reproduced. This result has been confirmed by Mori & Green (1976).

(iv) The compositions of the coexisting clinopyroxenes and orthopyroxenes lie off the ideal join $CaMgSi_2O_6$–$Mg_2Si_2O_6$ (i.e. the mineral phases are non-stoichiometric with respect to their Si/Ca + Mg) ratios). The solvus limits determined in this iron-free and alumina-free system are, therefore, dependent to a small degree upon the silica activity of the system, a

Table 1. Experiments at 20 and 30 kbar on gels with compositions on the join diopside (di)–enstatite (en) (results additional to those described by Howells & O'Hara (1975))

bulk composition of charge	Nature of starting material	*T*/°C	*P*/kbar	time/h	phases identified	comments
$di_{40}en_{60}$	gel recryst. to en_{ss} + cpx($di_{72.5}$)†	1450	30	0.33	opx + cpx($di_{64.7}$)	solution experiment
$di_{40}en_{60}$	gel recryst. to en_{ss} + cpx($di_{72.5}$)†	1450	30	4.08	opx + cpx($di_{63.3}$)	solution experiment
$di_{48.4}en_{51.6}$	gel recryst. to en_{ss} + cpx($di_{72.5}$)†	1450	30	4.25	opx + cpx($di_{66.7}$)	solution experiment
$di_{40}en_{60}$	gel	1400	30‡	17	opx + cpx($di_{66.7}$)	floating piston technique – as used by Davis & Boyd (1966)
$di_{48.4}en_{51.6}$	gel	1400	30‡	9.9	opx + cpx($di_{69.1}$)	
$di_{40}en_{60}$	gel	1600	20‡	0.5	cpx	two stage experiment which failed to reproduce results of similar experiment described in Kushiro (1969*b*)
$di_{40}en_{60}$	run product of previous experiment	1620	20‡	0.5	cpx	

† Recrystallization conditions were 1307 °C, atmospheric pressure, 14 d; total recrystallization to a fine grained intergrowth was achieved. Other gel starting materials had been partially crystallized at 900 °C, atmospheric pressure, for 24 h.

‡ Floating piston experiment: in all other experiments run conditions were attained as described in Howells & O'Hara (1975). All other experimental details are described in Howells & O'Hara (1975) and in the note above.

Further run details are described in Howells (1976).

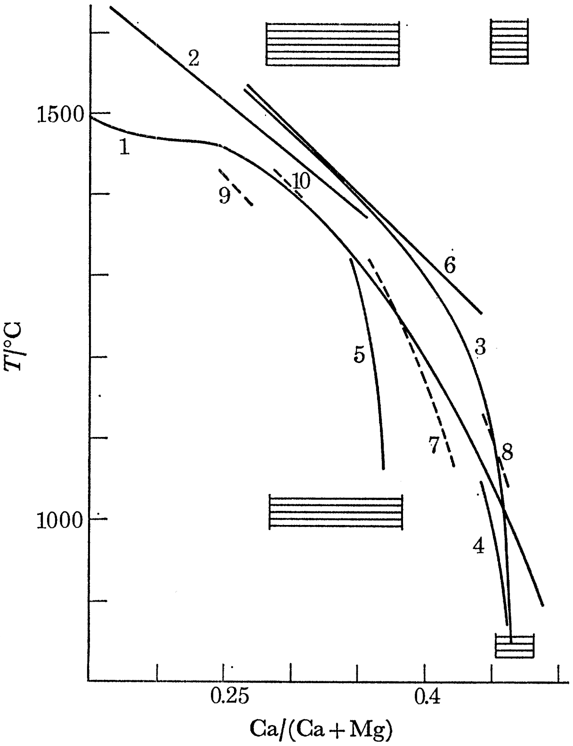

Figure 4. The diopside limb of the diopside–enstatite solvus – a selection of available determinations in the systems $CaO–MgO–SiO_2$, $CaO–MgO–Al_2O_3–SiO_2$ (solid curves) with some data from natural pyroxenes (broken curves) all projected into the diopside enstatite join as advocated by Boyd (1973). System $CaO–MgO–SiO_2$: 1, Davis & Boyd (1966), 30 kbar; 2, Howells & O'Hara (1975), 30 kbar; 3, Mori & Green (1975), 30 kbar; 4, Lindsley & Dixon (1976), 20 kbar. System $CaO–MgO–Al_2O_3–SiO_2$: 5, 6, Akella (1976), 26, 44 kbar respectively. Natural minerals: 7, 8, Akella (1976), 31, 38 kbar respectively; 9, 10, Hensen (1973), 27, 40.5 kbar respectively. The ranges of Ca/(Ca + Mg) ratio in natural clinopyroxenes from nodules in kimberlite are indicated by shaded regions at top and lower part of figure. Uncertainties in the estimated temperatures must now be regarded as large.

result confirmed by Mori & Green (1976). This effect leads to different compositions of the clinopyroxenes which coexist with enstatite being observed at the same temperature depending upon the differing Ca/(Ca + Mg) ratio of the starting mixtures in the join $CaMgSi_2O_6$–$Mg_2Si_2O_6$.

Some further data showing approach to the previously published solvus by solution of enstatite into diopside, rather than by exsolution of enstatite from diopside are presented in table 1. They again confirm the existence of the effect interpreted as due to non-stoichiometry of the pyroxenes.

Lindsley & Dixon (1976) doubted the existence of this effect of non-stoichiometry, but their results neither spanned the temperature range where the effect was observed by Howells & O'Hara (1975), nor reproduced the type of observation from which the effect was deduced (sensitive X-ray diffraction measurements recording the average Ca/(Ca + Mg) ratio of all clinopyroxene present in the run products from different initial starting compositions).

In figure 4 the Ca/(Ca + Mg) ratios of clinopyroxenes coexisting with enstatites in some more aluminous assemblages are also plotted. It is clearly unwise to ignore the effect of Al_2O_3 upon the diopside limb of the solvus when attempting to estimate temperatures.

Water content of runs as an explanation of non-stoichiometry

Lindsley & Dixon (1976) suggest that incomplete drying of the charges was the cause of the effects interpreted as due to non-stoichiometry of the pyroxenes (Howells & O'Hara 1975). The careful drying procedure adopted (Howells 1975) makes this improbable as an explanation of the effects. A similar drying technique was applied to diopside and pyrope used for calibration of temperature in the solid media equipment, both of which yielded sharp melting point phenomena without a significant range of partial melting below the solidus temperatures reported by other workers.

Implications of non-stoichiometry

Solvus limits which are intended for application to more complex mineral assemblages than the two or three phases directly concerned should be determined, or at least verified, in the presence of those other phases (Howells & O'Hara 1975). Effects of non-stoichiometry may become more serious as additional components are added to the system.

Nature of starting materials for experiments

The experiments next to be described, like those on the diopside–enstatite system mentioned above, have yielded results which are very different from those previously published by other workers (all of which were based directly or indirectly upon glass starting materials which had been prepared by repeated prolonged fusions of the oxides). It is important, therefore, to understand how the starting materials used at Edinburgh differed from other workers'.

The various types of starting material used in these studies are described in table 2. It will be apparent that our type A starting material is an ultrafine-grained oxide mix which has then been sintered at atmospheric pressure yielding a microcrystalline product. Type A material as there defined has previously been used in this laboratory to determine numerous relations. For example, many melting and subsolidus relations in the system CaO–MgO–Al_2O_3–SiO_2 are in excellent agreement with previously published data based directly or indirectly on glass starting materials (Humphries, Biggar & O'Hara 1972). Where discrepancies appeared, these have generally been resolved in favour of results based on type A starting materials.

TABLE 2. NATURE OF STARTING MATERIALS USED FOR EXPERIMENTS ON Al_2O_3 SOLUBILITY IN ORTHOPYROXENE AT THE EDINBURGH LABORATORY

type A	(crystallized gel) required oxide components coprecipitated as a gel, dried and NH_4NO_3 driven off to yield amorphous oxide mix, which then held at 500 °C for *ca.* 2 d, 900 °C for 1 d, milled, ground† to yield largely crystalline (< 1 μm crystal size, < 5 μm particle size) powder (see Biggar & O'Hara 1969*a* for further details). Dried‡
types B	(recrystallized gels)
type B_1	type A recrystallized 1200 °C for 1 month, 1 atm (*ca.* 10^5Pa) pressure (crystal size 1–2 μm, max. 8 μm), ground, dried
type B_2	type A recrystallized 1000 °C for 1 d, 1 kbar, *ca.* 5% H_2O (crystal size as type B_1), ground, dried
type B_3	type A recrystallized 1400 °C, 1 h, 30 kbar, damp§ (pyrope only)
type B_4	type A + seeds type B_3 recrystallized 1500 °C, 1 h, 30 kbar (pyrope only)
types C	
type C_1	type B_1 + 2% forsterite (type B_2) ground, dried
type C_2	type B_2 + 2% forsterite (type B_2) ground, dried
type C_3	type C_1 recrystallized at 1500 °C, 30 kbar, 4 h, ground and dried
type C_4	type C_2 recrystallized at 1500 °C, 30 kbar, 4 h, and again at 1500 °C, 30 kbar, 4.1 h
types D	(gel mixtures)
type D_1	$Wo_{5.5}En_{87}Alumina_{7.5}$ plus $Wo_{5.4}En_{90.1}Alumina_{4.5}$ both type A, mixed, ground, dried
type D_2	enstatite (type A) plus pyrope (type A) further recrystallized as under type B_2, ground, dried
type E	enstatite composition pyroxene crystals (type B_1) + pyrope crystals (type B_3) mixed, ground, dried. Crystal size 1–5 μm.
type F	enstatite crystals (type B_2) ± diopside crystals (type B_1) + pyrope crystals (type B_4) + forsterite crystals (type B_2) mixed, ground, dried
type G	type A converted to glass 1700 °C, 2–5 min, 1 atm in r.f. heater, dried (devitrified to < 0.1 μm pyroxene aggregate)
type H	type G recrystallized at 1350 °C, 9 h, 30 kbar, and at 1450 °C, 6.8 h, 30 kbar, mixed, ground, dried. Crystal size < 1 μm, garnet + enstatite
type J_1	bulk composition (type A or B_2) held 4 h at 1650 °C (above liquidus) at atmospheric pressure, then quenched to produce a glass with, it was hoped, little memory of the previous thermal history of the material. Believed to resemble the starting materials used by Boyd & England (1964), MacGregor (1974) and Akella (1976) more closely than any others used in these studies
type J_2	as J_1 but seeded with 1% previously synthesized pyrope crystals

† Ground = finely ground by hand under acetone in agate mortar to less than 5 μm particle size.

‡ Dried = dried at 1050 °C, 1–2 h, 1 atm pressure, welded immediately, loaded into furnace assembly, dried in dry N_2 flow, 900 °C for $\frac{1}{2}$ h. Pyrope crystals survived this treatment.

§ Damp = not dried after powder left in contact with laboratory atmosphere.

The new results which have been obtained for the solubility of alumina in orthopyroxenes coexisting with garnets in the systems $MgO–Al_2O_3–SiO_2$ and $CaO–MgO–Al_2O_3–SiO_2$ are themselves partly dependent upon the nature of the starting materials. These include gels of appropriate compositions which had been crystallized or recrystallized to varying extents at atmospheric pressure (types A, B_1, C_1) or at 1 kbar water vapour pressure (types B_2, C_2). Mixtures of crystallized gels (type D), and mixtures of pure and member crystals (types E, F) were also used. Material which had been converted to glass (types G and J) was also used. Some starting materials for the results quoted finally had been previously run at high pressure and temperature (types C_3, C_4).

The experiments whose results are listed in table 3 have concentrated mainly on the situation at or about 1500 °C, 30 kbar pressure, where it might have been anticipated that rates of

Table 3. Results of runs on Al_2O_3 solubility in orthopyroxene

(Unless otherwise stated, all run materials were dried (see table 2, footnote ‡).)

composition (all in mass percentages)	material type	P/kbar	T/°C	time/h	nature of experiment	results
I. system $MgO–Al_2O_3–SiO_2$						
1. relevant to the *ca.* 8 mass % Al_2O_3 isopleth						
enstatite$_{68}$ pyrope$_{32}$ equivalent to enstatite$_{91.9}$ alumina$_{8.1}$	type D_2	30†	1650	0.5	synthesis	opx; Δ gives‡ 8.3, 8.6 % Al_2O_3
		30	1550	2.2	synthesis	opx, (gt); Δ gives 8.0, 8.6 % Al_2O_3
		30	1400	6.2	synthesis	opx, gt; Δ gives 6.7, 6.8 % Al_2O_3
		27	1480	4.3	synthesis	opx, gt; Δ gives 8.0, 8.6 % Al_2O_3
		30§	1480	4.0	synthesis	opx, gt
	type E	30	1550	2.0	solution	opx, gt; Δ gives 7.5, 8.8 % Al_2O_3
	type J_1	30	1500	0.01	synthesis	opx, (?sp)
	type J_1	30	1500	4.0	synthesis	opx, (gt)
	type J_1 damp	30	1500	24.0	synthesis	opx, gt
	type J_2 damp	30	1500	4.0	exsolution	opx, gt
	type J_2 damp	30	1500	24.0	exsolution	opx, gt
2. relevant to the *ca.* 5 mass % Al_2O_3 isopleth (wet or damp)						
enstatite$_{80}$ pyrope$_{20}$ equivalent to enstatite$_{94.9}$ alumina$_{5.1}$	type B_1 damp‖	29.1	1150	17.0	synthesis	unrecrystallized (opx)
	type $B_1 + 2.5\,\%\ H_2O$	29.4	1100	15.5	synthesis	opx, gt
	type $B_1 + 4.0\,\%\ H_2O$	30.0	1174	17.0	synthesis	opx, q
	type $B_1 + 6.7\,\%\ H_2O$	30.4	1200	18.0	synthesis	opx, q, (gl, ol)
	type $B_2 + 5.3\,\%\ H_2O$	30	1050	24	synthesis	opx, gt (4.1 %)
II. system $CaO–MgO–Al_2O_3–SiO_2$						
1. relevant to the 7.5 mass % Al_2O_3 isopleth						
Wo$_{5.5}$ En$_{87}$ alumina$_{7.5}$	type A	30	1600	0.7	synthesis	opx, (cpx), gt
	type A	30	1500	4.1	synthesis	opx, (cpx), gt
	type C_2 damp	30	1500	24	synthesis	opx, (cpx?), gt (5.8 %)
2. relevant to the 6 mass % Al_2O_3 isopleth						
(*a*) no excess forsterite						
Wo$_{5.4}$ En$_{88.6}$ alumina$_{6.0}$	type D_1	35	1660	0.3	synthesis	opx, (cpx)
		35	1620	0.4	synthesis	opx, gt, (cpx)
		35	1580	1.5	synthesis	opx, gt, (cpx)
		30	1565	2.0	synthesis	opx, (cpx)
		30	1542	2.6	synthesis	opx, gt, (cpx)
		30	1523	3.8	synthesis	opx, gt, (cpx)
		27	1520	3.5	synthesis	opx, (cpx?)
		27	1480	5.3	synthesis	opx, gt, (cpx)
Wo$_{6.5}$En$_{87.5}$ alumina$_{6.0}$	type B_1	30	1550	2.5	synthesis	opx, (gt), (cpx)
		30	1534	2.0	synthesis	opx, gt, (cpx)
(*b*) excess forsterite present						
(Wo$_{6.5}$ En$_{87.5}$ alumina$_{6.0}$)$_{98}$ + forsterite$_2$	type C_1	30	1565	2.4	synthesis¶	opx, (cpx), (ol)
		30	1550	1.5	synthesis	opx, gt, (cpx), (ol)
		30	1500	4.0	synthesis	opx, gt, (ol), (cpx?)
	type C_3	30	1500	4.1	exsolution	opx, gt, (ol), much more garnet than in preceding experiment
	type C_1	30	1500	0.01	synthesis	opx, ((gt)), (ol), (?cpx)
	type C_2	30	1500	0.01	synthesis	opx, (gt), (ol), (?cpx) (4.2–8.6 %)
	type C_2 damp††	30	1500	4.0	synthesis	opx, ((Gt)), (ol, cpx) large opx prisms (5.7 %)
	type C_4	30	1500	4.0	exsolution	opx, gt, (ol, cpx) common euhedral garnet (6.2 %)

TABLE 3 (*cont.*)

composition (all in mass percentages)	material type	*P*/kbar	*T*/°C	time/h	nature of experiment	results
II. system CaO–MgO–Al$_2$O$_3$–SiO$_3$ (*cont.*)						
(Wo$_{6.5}$ En$_{8.75}$ alumina$_{6.0}$)$_{98}$ + forsterite$_2$	type C$_2$	30	1500	24	exsolution	opx, gt, cpx, ol (5.9%)
	type C$_2$	30	1500	67	exsolution	opx, gt, cpx, ol (5.7%)
	type C$_2$ damp	30	1500	24	exsolution	opx, gt, cpx, ol‡‡ (5.4%)
	type C$_2$ damp	30	1600/ 1500	4/20	exsolution	opx, gt
	type F	30	1500	0.01	solution	opx, gt, (ol, cpx)
	type F	30	1500	4.0	solution	opx, (gt), (ol, cpx) (4.5%)
	type F damp	30	1500	4.0	solution	opx, ((gt)), (ol, cpx) (5.6%)
	type F damp	30	1500	24.0	solution	opx, gt, cpx, ol‡‡ (5.6%)
	type C$_2$ + 5% H$_2$O	30	1050	24.0	synthesis	opx, gt, cpx, ol (2.45%)
	type J$_1$	30	1500	4.0	synthesis	opx
	type J$_1$ damp	30	1500	4.0	synthesis	opx
	type J$_1$ damp	30	1500	24.0	synthesis	opx, (gt)
	type J$_2$ damp	30	1500	4.0	exsolution	opx, gt
	type J$_2$ damp	30	1500	24.0	exsolution	opx, gt
3. relevant to the 4½ mass % Al$_2$O$_3$ isopleth						
(*a*) no excess forsterite						
Wo$_{5.4}$ En$_{90.1}$ alumina$_{4.5}$	type B$_1$	30	1525	2.4	synthesis	opx, (cpx?)
		30	1498	4.4	synthesis	opx, (gt)§§, (cpx?)
	type A	30	1450	4.7	synthesis	opx, ((gt)), (cpx?)
	type G	30	1450	6.8	synthesis	opx, (?cpx)
		30	1350	9.0	synthesis	opx, (gt), (?cpx)
	type H	30	1450	6.0	exsolution	opx, gt, (?cpx) much more garnet apparent than in 2 preceding runs
(*b*) excess forsterite present						
(Wo$_{5.4}$ En$_{90.1}$ alumina$_{4.5}$)$_{90}$ + forsterite$_{10}$	type B$_1$	30	1525	1.9	synthesis	opx, (gt)§§, ol, (cpx)
		30	1500	4.3	synthesis	opx, (gt)§§, ol, (cpx)
		30	1465	6.0	synthesis	opx, gt, ol, (cpx)
		30	1350	6.4	synthesis	opx, gt, ol, (cpx)
	type C$_2$ damp	30	1500	4	synthesis	opx, ol, cpx (4.3%)
	type C$_2$	30	1500	24	synthesis	opx, ol, cpx (4.7%)
	type C$_2$ damp	30	1500	24	synthesis	opx, ol, cpx (4.6%)

Key to phases identified: opx = orthopyroxene; gt = garnet; q = quench (chiefly pyroxene); gl = glass; ol = olivine; cpx = clinopyroxene (Ca-rich). Phase is in parentheses if present in very small amounts.

† All pressures, unless otherwise stated, were attained by piston out procedures, i.e. to desired pressures + 5 kbar, to temperature, then immediately lower to desired run pressure. Garnet nucleation will be favoured by the approach procedure. Temperatures were controlled and measured using Pt–Rh thermocouples (up to 18 h in low temperature runs) or W–Re thermocouples (in all runs of *ca.* 24 or more hours duration, and some at higher temperatures).

‡ Δ is measurement of $\Delta 2\theta$ for orthopyroxene X-ray reflections, as described by Boyd & England (1960). Figures in parentheses record mass % Al$_2$O$_3$ in orthopyroxenes based on electron microprobe data. Accuracy is manifestly no better than ± 0.2%.

§ Floating piston experiment. Pressures attained by pumping to pressure, raising to temperature, keeping at desired pressure throughout.

|| See table 2, footnote §.

¶ Other experiments (below) for this composition demonstrate that the low pressure mineral assemblage has largely or completely converted to a range of aluminous orthopyroxene compositions with a very few tiny garnets after *ca.* 30 s at 30 kbar, 1500 °C. Many of the experiments listed here as 'syntheses' are in practice exsolution combined with homogenization experiments in which garnet has formed from an aluminous enstatite composition during the greater part of the duration of the experiment.

†† Damp here means dried only at 135 °C, 2 min after prolonged exposure to the laboratory atmosphere.

‡‡ Analyses of constituent minerals in table 4.

§§ The 'garnets' recorded in these runs were very scarce, irregular and very small. They neither increased in amount nor attained subhedral or euhedral forms in longer runs, with or without moisture present. The interpretation offered in this paper does not regard these as present at equilibrium in this bulk composition at the relevant pressures and temperatures.

reaction and equilibration would have been comparatively rapid. Previous experience in these systems had suggested that solution of garnet into orthopyroxene is a rapid process, whereas nucleation and growth of garnet from aluminous enstatite is a slow or erratic process (Boyd & England 1964). The situation found in these experiments when combined with data from previous workers is clearly complex.

Figure 5 shows the results of experiments at 1500 °C, 30 kbar to determine Al_2O_3 solubility in enstatite coexisting with garnet, diopside-rich pyroxene, and in most cases forsterite, in the system $CaO–MgO–Al_2O_3–SiO_2$. Using a particular type of starting material (for example, the long-annealed glass based starting materials used by Akella (1976)) it is possible to approach a particular solubility limit (*ca.* 7.1 % Al_2O_3) by exsolving garnet from aluminous orthopyroxenes within about 3 h. Using a different starting material, one which has never been converted to glass, it is possible to approach a different solubility limit (*ca.* 5.5 % Al_2O_3). This can be done by dissolving garnet into orthopyroxene, and by growing garnet from a charge which initially developed a range of relatively aluminous enstatite compositions. Convergence on this value is rapid (less than 4 h) in charges which contained a little moisture, but is more sluggish in charges which had been thoroughly dried.

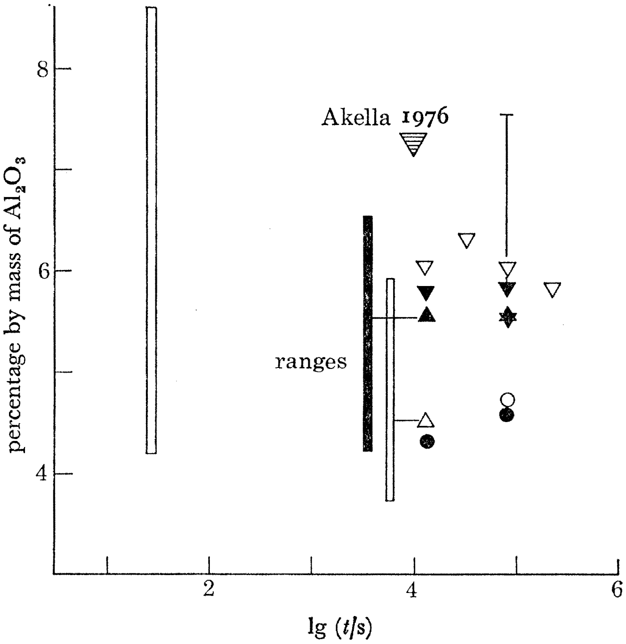

FIGURE 5. Alumina content of enstatites grown in experiments at 30 kbar, 1500 °C, as a function of time and starting material, indicating the direction of approach to the measured alumina contents, all of which are based on electron microprobe data. The result by Akella (1976) was based on starting materials originally derived from glass. Results for 6 % Al_2O_3 composition are shown by triangles, those for the 4.5 % Al_2O_3 composition by circles. Solid symbols represent the results from damp runs, open symbols the results from dry runs. The ranges of individual point analyses in two solution experiments of 4 h duration which had clearly not reached equilibrium, and in a 30 s synthesis experiment are indicated.

The pattern of results can be interpreted in terms of the interplay of three factors:

(i) reluctant nucleation of garnet from aluminous orthopyroxene especially in dry charges, but relatively rapid solution of garnet into orthopyroxene,

(ii) 'equilibration' of the Al_2O_3 content of orthopyroxene of a given structural state (despite the circumstances noted in (i)) at a faster rate than

(iii) adjustment of the structural state of the orthopyroxene, with consequent change of the solubility limits of Al_2O_3 in the slowly changing orthopyroxene structure.

Our data do not preclude, and may yet require, the operation of another effect. The structural state of the orthopyroxene produced initially under any particular conditions of pressure and temperature may be partly dependent upon the bulk composition of the charge from which it has grown. The results which point to this possibility are observations on types A and B_1 starting materials on the 4.5, 6.0 and 7.5 % Al_2O_3 compositions in the system CaO–MgO–Al_2O_3–SiO_2. Small amounts of garnet grow in all these charges at 1400–1500 °C, 30 kbar, but the relative amounts of garnet are apparently not compatible with a unique value of Al_2O_3 in the orthopyroxenes grown from the different charges (although all contain forsterite, garnet and two pyroxenes). Similar results have been observed in charges having the bulk compositions of the clinopyroxenes which may coexist with these orthopyroxenes (Howells 1976).

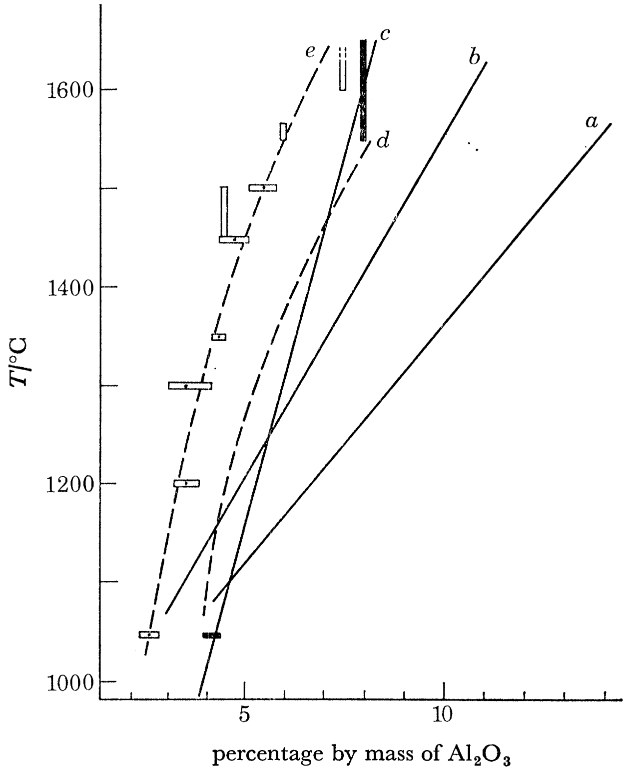

FIGURE 6. Alumina contents of enstatite coexisting with garnet in the systems MgO–Al_2O_3–SiO_2 (solid lines and ornaments: *a*, Boyd & England 1964; *b*, MacGregor 1974; *c*, new data) and CaO–MgO–Al_2O_3–SiO_2 (broken lines and open ornaments: *d*, Akella 1976; *e*, new data) as a function of temperature at 30 kbar pressure. Note the revision to some previously published data points (Howells 1975) at or near 1500 °C, 4.5 % Al_2O_3. Horizontal bars indicate the range of Al_2O_3 contents reported in individual microprobe analyses of experimental charges. Runs at 1450–1200 °C are not detailed in table 3, but were 24–72 h runs on damp type C_2 starting materials.

However, the results represented in figure 5 and other data represented in figures 6 and 7 concur in showing that at high temperatures garnet will coexist for long times with orthopyroxenes which contain much less alumina than the limits set by the data of Akella (1976) or MacGregor (1974). The longer the duration of these experiments, the lower the Al_2O_3

contents of the orthopyroxenes become. This suggests the interpretation that these low values of Al_2O_3 solubility are closer to, but probably higher than, the true equilibrium values in orthopyroxenes of the correct structural states.

As a confirmation of the reversibility of the low solubility limit of alumina in enstatite at 1500 °C, 30 kbar, an experiment was carried out on the 6 % Al_2O_3 mixture in the system $CaO–MgO–Al_2O_3–SiO_2$, holding it first at 1600 °C, 30 kbar for 4 h (when no garnet forms), then for a further 20 h at 1500 °C (without intermediate quenching of the charge). Garnet had formed in the run products although (visual estimate) the amount was less than in many of the other runs, and the Al_2O_3 content of the enstatite must be close to 5.9 %.

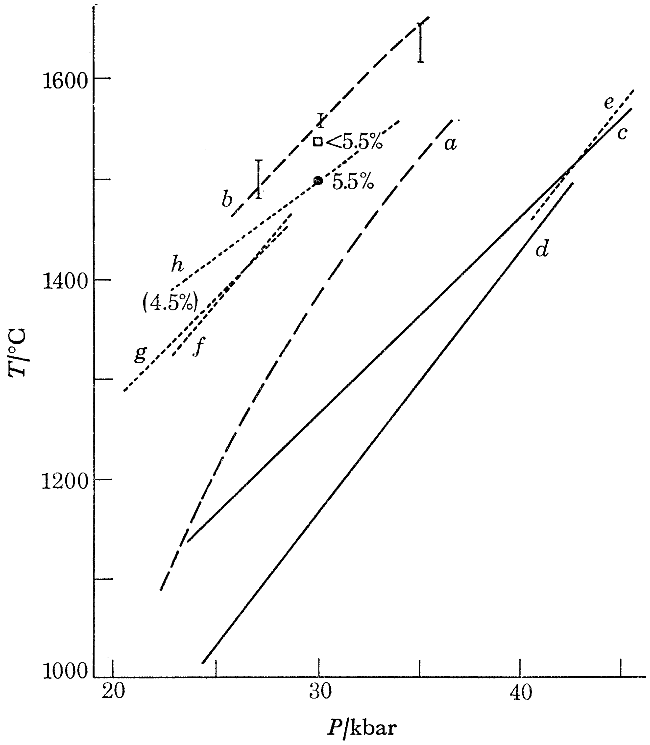

Figure 7. Plot of temperature against pressure comparing the published isopleths of 6 % alumina (by mass) content in enstatites coexisting with garnet in some synthetic and natural systems in relation to the new data. Broken lines show the isopleths for 6 % Al_2O_3 in the system $CaO–MgO–Al_2O_3–SiO_2$ as determined (*a*) by Akella (1976) and (*b*) in the present study. A relatively steep slope has been chosen arbitrarily to fit the new data. Solid lines show similar isopleths for the system $MgO–Al_2O_3–SiO_2$ as determined by (*c*) MacGregor (1974) and (*d*) Boyd & England (1964). The position of the well established data point (see figure 5) at 30 kbar, 1500 °C, is shown by the filled circle. Dotted lines show the positions of the isopleths for 6 % Al_2O_3 in natural orthopyroxenes equilibrated with garnets in three previous studies. (*e*, MacGregor & Ringwood 1964; *f*, Green & Ringwood 1970; *g*, Hensen 1973). Also shown in the 4.5 % Al_2O_3 isopleth (*h*) from Akella (1976). The open square shows a datum point from the natural sample 1031 (Howells *et al.* 1975) whose lack of agreement with previous results prompted the present studies; this datum point is in satisfactory agreement with Akella's (1976) data for natural mineral assemblages, and with the new data for the system $CaO–MgO–Al_2O_3–SiO_2$.

The final tests which were carried out were to determine the reasons for the discrepancy between our data and those obtained by previous workers, and the relative stability of the alternative results. Glass starting materials (type J) were prepared in a manner such as to resemble as closely as possible the physical state of the starting materials used by Boyd &

PHILOSOPHICAL TRANSACTIONS OF THE ROYAL SOCIETY A MATHEMATICAL, PHYSICAL & ENGINEERING SCIENCES

England (1964), MacGregor (1974) and Akella (1976). The 8% Al_2O_3 composition on the enstatite–pyrope join, and the 6% Al_2O_3 composition in the enstatite–diopside–pyrope–forsterite system were prepared in this way. Neither should contain garnet at equilibrium at 1500 °C, 30 kbar, according to the previously published data; both should contain garnet according to the new data (see figure 6). Neither yielded garnet in the run products after 30 s duration at 1500 °C, 30 kbar, nor after 4 h in the case of the 6% Al_2O_3 composition. The 8% Al_2O_3 composition had nucleated garnet after 4 h, and both compositions contained garnet after runs of 24 h duration. When these same glass starting materials were seeded with 1% by weight of presynthesized pyrope crystals, much more garnet was observed in the run products after 4 and 24 h on both compositions.

These run durations are much longer than had previously been used at this temperature and the discrepancy between different workers results must be set down to the adverse effects of one or more of the three factors listed above. The low alumina solubilities in enstatite at 1500 °C which are reported in this paper represent a closer approach to the equilibrium values.

Some comments on gel and glass as starting materials

Starting materials based on glasses prepared by long heating performed relatively poorly in the experiments described above, when compared with reaction rates in starting materials prepared from gels.

The very fine grained crystalline starting materials which are obtained from the gels (e.g. types A, B_1, B_2 of table 1) have also proved more favourable than glass-based starting materials for the establishment of non-stoichiometry and solubility limits in diopside (Biggar & O'Hara 1969*a*, *b*); non-stoichiometry of monticellite and solubility limits in the monticellite–forsterite solvus (Biggar & O'Hara 1969*b*); the stability of diopside plus spinel rather than anorthite, forsterite and melilite at atmospheric pressure (O'Hara & Biggar 1969); and the effects of temperature, pressure, and non-stoichiometry upon the solubility of enstatite in diopside (Howells & O'Hara 1975).

Glass-based starting materials had previously yielded metastably high solubility limits for both alumina and enstatite in diopside during devitrification at atmospheric pressure, much lower limits being determined after long heating close to the solidus (O'Hara & Schairer 1963). Subsequently studies on these solubility limits using crystallized gel starting materials have yielded still lower solubility limits (unpublished data).

Pyroxene compositions grown from crystallized gel starting materials (which are essentially very fine grained oxide mixes in the early stages of their preparation) show persistently lower limits of solubility towards both alumina and the other pyroxene than are obtained from short experiments on dry glass-based starting materials. Other results on glass-based materials or oxide mixes using long run times or hydrothermal conditions have confirmed these lower solubility limits in pyroxene (e.g. Mori & Green 1975, 1976; Lindsley & Dixon 1976).

Glass does not, therefore, seem to be the ideal starting material for subsolidus equilibrium experiments.

PREFERRED VALUES OF Al_2O_3 SOLUBILITY IN ENSTATITE COEXISTING WITH GARNET

Electron microprobe analyses of forsterite, garnet, orthopyroxene and clinopyroxene from the relatively coarse-grained products of a 24 h run on damp starting material are quoted in table 4. These compositions are contrasted with results quoted by Akella (1976) for the same conditions, the difference in the clinopyroxene compositions being particularly striking.

Preliminary data for some experiments carried out in the presence of relatively large amounts of water at *ca.* 1050 °C are also reported in table 3, and represented in figures 6 and 8.

TABLE 4. COMPOSITIONS OF MINERALS IN EXPERIMENTS AT 1500 °C, *ca.* 30 kbar PRESSURE AS INDICATED IN TABLE 3

mineral	experimental type	SiO_2	Al_2O_3	MgO	CaO
orthopyroxene	(exsolution)	56.13	5.36†	35.98	2.20
	(solution)	56.01	5.58	35.79	2.28
	(Akella 1976)‡	55.2	7.1	35.4	2.3
clinopyroxene	(exsolution)	53.54	5.44	24.12	17.15
	(solution)	53.54	5.77	23.95	16.64
	(Akella 1976)‡	49.8	12.2	22.6	15.1
garnet	(exsolution)	45.12	23.49	25.64	5.72
	(Akella 1976)‡	44.7	23.8	26.1	5.4
olivine	(exsolution)	42.76	0.22	57.21	0.24

† Simultaneous solution of Powell's (1978) equations for Ca–Mg distribution between two pyroxenes and garnet yields 1446 °C, 29.6 kbar, for the average pyroxene compositions. Wood & Bannos' (1973) equations yield an estimate of 1575 °C, 38.2 kbar while Wood & Banno (1973) combined with Wood (1974) yields an estimate of 1575 °C, 35.2 kbar.

‡ Results quoted were at 31 kbar.

If these results can be taken to approximate to equilibrium and are combined with the *ca.* 1500 °C data, they imply that $\mathrm{d}T/\mathrm{d}P$ of the isopleths of alumina solubility in orthopyroxene coexisting with garnet in the system $MgO–Al_2O_3–SiO_2$ is greater than hitherto believed. The steep, curved solubility limits found in the system $CaO–MgO–Al_2O_3–SiO_2$ by Akella (1976) are confirmed.

APPLICATIONS OF THE RESULTS

Figure 8 illustrates the relation between temperature of equilibration (controlled or inferred) and the alumina contents of some experimentally produced and some natural orthopyroxenes coexisting with garnets from garnet–lherzolite facies xenoliths in kimberlites and from granulite facies gneisses at Scourie, NW Scotland. In the case of the orthopyroxenes from xenoliths in kimberlites, there are comparable amounts of Cr_2O_3 and some Fe_2O_3 which must be taken into account when interpreting the Al_2O_3 contents of these pyroxenes. This problem is less severe in the case of the granulite facies pyroxenes from Scourie where aluminium appears to be the dominant trivalent cation in the structures.

Figure 8 shows that considerable extrapolation of all the experimental results is necessary before they can be applied to natural materials. Consequently the uncertainty in the estimated pressures will be relatively large.

However, reduced solubility limits of alumina in orthopyroxene at high temperatures have been reported in this paper. The effect of this must be to reduce all pressure estimates for high temperature assemblages such as some of those from xenoliths in kimberlite. Revisions to the diopside–enstatite solvus have already tended to raise the estimated temperatures of equilibration of such assemblages. The effect of the revisions will be to yield points on inferred palaeogeotherms which indicate higher temperatures at shallower depths than has hitherto been believed.

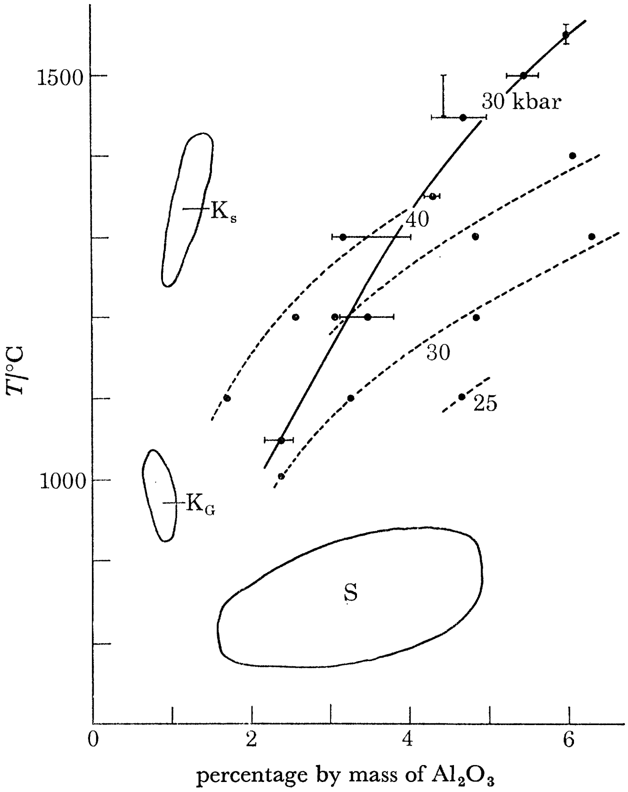

Figure 8. Plot of temperature against alumina contents of orthopyroxenes coexisting with garnets in some natural parageneses from sheared (K_s) and granular (K_G) nodules in kimberlites and granulite facies gneisses from Scourie (S) (temperature estimates from Boyd (1973) and application of the Wood & Banno (1973) pyroxene geothermometer respectively). The positions of the isopleths of alumina content actually determined in experimental studies by MacGregor (1974) in the system $MgO–Al_2O_3–SiO_2$ are shown by dotted lines. That determined at 30 kbar in the present study is shown by the solid line.

The relatively gently sloping (low dT/dP) isopleths of alumina solubility in orthopyroxene which were established by the experimental studies of Boyd & England (1964) and MacGregor (1974) may be extrapolated to lower temperatures using the thermodynamic arguments of Wood & Banno (1973) and Wood (1974). If the isopleths are in fact steeper (higher dT/dP), and have comparable values of pressure at 1200 °C (see figure 6) to those previously reported, they will predict the presence of more alumina than hitherto expected in orthopyroxenes equilibrated with garnets at still lower temperatures. Application of the Wood–Banno (1973) and Wood (1974) geobarometers to such mineral assemblages would therefore yield pressure estimates which are too low. This is the type of discrepancy actually observed in a test case (O'Hara & Yarwood 1978, this volume, table 2).

Conclusions

Spurious changes of slope of apparent geotherms obtained from peridotite nodules in kimberlites may arise if the curvature of the solvus limb assumed in order to estimate the temperatures, or of the Al_2O_3 isopleths assumed in order to estimate the pressures differs from that of the true equilibria. Revisions to the diopside–enstatite solvus indicate that lower temperatures on published geotherms should be adjusted downwards while higher temperatures should be adjusted upwards. However, all estimates are subject to considerable uncertainties unless the effects of pressure and Al_2O_3 content of the pyroxenes are taken into account, as well as possible effects of silica-activity and non-stoichiometry of the pyroxenes. Revisions to the enstatite–pyrope solvus indicate that estimated pressures (depths) may require to be adjusted to lower values in the high temperature range; the estimates at lower temperatures appropriate to crustal gneisses may, however, have to be revised in the opposite sense.

References (Howells & O'Hara)

Akella, J. 1976 *Am. Miner.* **61**, 589–598.

Biggar, G. M. & O'Hara, M. J. 1969*a* *Progress in experimental petrology, 1st report*, pp. 86–96. London: Natural Environment Research Council.

Biggar, G. M. & O'Hara, M. J. 1969*b* *J. Am. ceram. Soc.* **52**, 249–252.

Boyd, F. R. 1973 *Geochim. cosmochim. Acta* **37**, 2533–2546.

Boyd, F. R. & England, J. L. 1960 *Carnegie Instn Wash. Yb.* **59**, 47–52.

Boyd, F. R. & England, J. L. 1964 *Carnegie Instn Wash. Yb.* **63**, 157–161.

Davis, B. T. C. & Boyd, F. R. 1966 *J. geophys. Res.* **71**, 3567–3576.

Green, D. H. & Ringwood, A. E. 1970 *Phys. Earth planet. Int.* **3**, 359–371.

Hensen, B. J. 1973 *Carnegie Instn Wash. Yb.* **72**, 527–534.

Howells, S. 1975 *Ext. Abstracts, Int. Conf. on Geothermometry and Geobarometry*. Pennsylvania State University.

Howells, S. 1976 Ph.D. thesis, Edinburgh University.

Howells, S., Begg, C. & O'Hara, M. J. 1975 *Phys. Chem. Earth* **9**, 895–902.

Howells, S. & O'Hara, M. J. 1975 *Nature, Lond.* **254**, 406–408.

Humphries, D. J., Biggar, G. M. & O'Hara, M. J. 1972 *Progress in Experimental Petrology*. Natural Environment Research Council Publ., Ser. D, **2**, 138–139.

Kushiro, I. 1969*a* *Carnegie Instn Wash. Yb.* **67**, 80–83.

Kushiro, I. 1969*b* *Am. J. Sci.* **267** A, 269–294.

Lindsley, D. H. & Dixon, S. A. 1976 *Am. J. Sci.* **276**, 1285–1301.

MacGregor, I. D. 1974 *Am. Miner.* **59**, 110–119.

MacGregor, I. D. 1975 *Phys. Chem. Earth* **9**, 455–466.

MacGregor, I. D. & Ringwood, A. E. 1964 *Carnegie Instn Wash. Yb.* **63**, 161–163.

Mori, T. & Green, D. H. 1975 *Earth planet. Sci. Lett.* **26**, 277–286.

Mori, T. & Green, D. H. 1976 *Am. Miner.* **61**, 616–625.

Nehru, C. E. & Wyllie, P. J. 1974 *Contr. Miner. Petr.* **48**, 221–228.

O'Hara, M. J. 1975 *Ext. Abstracts, Int. Conf. on Geothermometry and Geobarometry*. Pennsylvania State University.

O'Hara, M. J. & Biggar, G. M. 1969 *Am. J. Sci.* **267** A, 364–390.

O'Hara, M. J. & Schairer, J. F. 1963 *Carnegie Instn Wash. Yb.* **62**, 107–115.

O'Hara, M. J & Yarwood, G. 1978 *Phil. Trans. R. Soc. Lond.* A **288**, 441–456 (this volume).

O'Hara, M. J. & Yoder, H. S. Jr 1967 *Scott. J. Geol.* **3**, 67–117.

Powell, R. 1978 *Phil. Trans. R. Soc. Lond.* A **288**, 457–469 (this volume).

Wood, B. J. 1974 *Contr. Miner. Petr.* **46**, 1–15.

Wood, B. J. & Banno, S. 1973 *Contr. Miner. Petr.* **42**, 109–124.